First-principles simulations of metal-ceramic interface adhesion: Co/WC versus Co/TiC

Mikael Christensen, Sergey Dudiy,* and Göran Wahnström
Department of Applied Physics, Chalmers University of Technology and Göteborg University, SE-412 96 Göteborg, Sweden
(Received 23 July 2001; revised manuscript received 15 October 2001; published 2 January 2002)

With the purpose to understand the fundamental difference between two industrially important classes of hard materials, WC-Co cemented carbides and TiC-Co cermets, we do a comparative study of Co/WC and Co/TiC interface adhesion. Using first-principles density-functional plane-wave pseudopotential calculations, we analyze the energetics and electronic structure of the Co/WC interface, and compare with previously reported results for Co/TiC. Values for the work of separation and the interface energy are provided for a set of model Co(001)/WC(001) interfaces with fcc Co and cubic WC, which is a relevant case in sintering of Ti(W)C-Co cermets. The known fact of better wetting for Co on WC than on TiC is confirmed and explained in terms of the electronic structure. Both Co/WC and Co/TiC are characterized by strong covalent Co-C interface bonds. The stronger adhesion in the Co/WC case originates from a larger contribution of the Co-W metal-metal bonding rather than from the Co-C bonds.

DOI: 10.1103/PhysRevB.65.045408 PACS number(s): 68.35.−p, 71.15.Nc

I. INTRODUCTION

Metal-ceramic interfaces play a vital role in a wide variety of industrial applications, from light bulbs to microelectronic components and medical implants. The distinct nature of the contacting materials also makes metal-ceramic systems of much scientific interest, as reflected in an increasing number of experimental and theoretical studies.[1,2] The progress in this area has been particularly rapid in recent years. On the one hand, this is due to more refined experimental techniques becoming available to explore the interface atomic and electronic structures (see, e.g., Refs. 3 and 4). On the other hand, the development of theoretical models, such as density-functional theory, and the rapidly increasing performance of computers have made it possible to approach these kind of problems with direct first-principles calculations.[5–15]

An important class of metal-ceramic interfaces is those in composite materials. Composites are heterogeneous mixtures of dissimilar materials that perform considerably better than any of their components by itself. A particular case of composites of interest in this study are hardmetals, such as WC-Co cemented carbides and Ti(C,N)-Co cermets,[16,17] which are among the most common cutting-tool materials in the modern industry. These composite materials consist of grains of carbides or carbonitrides glued with a binder metal to combine the hardness of the carbide with the toughness of the metal. They are typically produced by liquid-phase sintering of the carbide and metal powders.

To optimize the mechanical properties of hardmetals it is important to have a good understanding of the internal heterointerfaces. For example, higher adhesion between the metal and ceramic gives an improved load transfer, higher yield strength, and stiffness.[18] The interface energetics controls different aspects of hardmetal sintering, such as wetting of hard grains by liquid binder, as well as microstructural changes during dissolution and reprecipitation processes. In other words, the success of any particular metal-carbide combination must ultimately be found in the metal-carbide interaction at the interface between the grains and the binder phase.

A representative case of hard metal interfaces, the Co/Ti(C,N) system, is addressed in a recent work.[19–21] With the help of first-principles density-functional calculations, it is shown that the Co/Ti(C,N) adhesion is mainly due to a special kind of Co-C(N) covalent bonds, which are noticeably stronger than Co-C(N) or Ti-C(N) bonds in bulk Co(C,N) or Ti(C,N). With a simple treatment of the interface structural irregularities, those calculations reproduce reasonably well the wetting experiment data for liquid Co on TiC. The present paper considers another important situation of hard metal interfaces, in particular the Co/WC system.

Although Ti(C,N)-based cermets play an increasing role in high-performance cutting, they are more brittle than the traditional WC-Co cemented carbides, and hence are less suitable for rough cutting. As a consequence, the tool market is still dominated by the WC-Co cemented carbides. Moreover, even in cermets it is typically necessary to have W in the carbide grains to provide sufficient wetting of the grains by the binder. In this situation, the development of hard materials could benefit significantly from fundamental understanding of what makes WC so successful, and what is behind the common differences between the WC-Co cemented carbides and Ti(C,N)-Co cermets. In answering these questions, a systematic comparison of Co/WC and Co/TiC interface adhesion is a natural first step.

The present paper aims at a systematic study of the Co/WC interface energetics and electronic structure. It also compares our results for the Co/WC interface to the previously studied Co/TiC case and in this way provides microscopic-level insight into the fundamental differences between the WC-Co cemented carbides and the TiC-Co cermets.

The paper is organized as follows. The next section gives a description of the computational method used, followed by the results and discussion for the bulk phases and the interface systems. Section III summarizes our conclusions.

II. RESULTS AND DISCUSSION

Our total-energy and electron-structure calculations are done in the framework of the density-functional theory.[22–24]

The exchange-correlation is treated at the generalized gradient approximation (GGA) level, version Perdew-Wang 91 (Ref. 25) (GGA-PW91). We use the DACAPO code,[26] which is an implementation of the plane-wave pseudopotential (PWPP) method.[27–30] The ion cores are described within the Vanderbilt ultrasoft pseudopotential scheme,[31] including the nonlinear core corrections[32] for Co and W. Good total-energy convergence, within 0.01 eV/atom, is reached with the plane-wave cutoff 26 Ry. The Brillouin zone is sampled using the Monkhorst-Pack method.[33] To improve the *k*-point convergence, the Fermi discontinuity is smeared according to the Gillan scheme,[34] with an effective electronic temperature 0.15 eV. The atomic structure relaxation is performed with the Broyden-Fletcher-Goldfarb-Shanno quasi-Newton method,[35] using the Hellman-Feynman theorem for the ionic force calculation. The ionic positions are optimized until the total residual force is less than 0.1 eV/Å.

A. Bulk phases

In contrast to the NaCl structure of the group-IVB metal carbides (e.g., TiC), the ground-state crystalline form of pure WC is hexagonal (see, e.g., Ref. 16). This form is observed over the whole temperature interval relevant for hard metal sintering (below 2000 °C). However, as a first step towards understanding the difference between the Co/WC and Co/TiC adhesion, we analyze the situation when the WC bulk phase has the same NaCl structure as TiC. This should greatly simplify the comparison with the preceding Co/TiC study.[19–21] At the same time, the NaCl phase of WC, known as its β phase, can be obtained experimentally at sufficiently high temperatures (above 2500 °C),[36] and can be stabilized even at room temperature.[37] In addition, the case of interfaces with NaCl WC and TiC phase is interesting for understanding the adhesion of Co to an mixed (W,Ti)C phase. Even at relatively low Ti concentrations that phase also has a NaCl structure.[38] Such a mixed case reflects the situation in the Ti(W)C-Co cermets, at the boundaries between the Co binder and the (W,Ti)C rim of the hard carbide grains (see, e.g., Ref. 39).

The Co phase is taken to be fcc, which is a very realistic situation for sintered carbides.[40] Only the case of paramagnetic Co is considered. This should be a more relevant situation in the context of wetting, i.e., above the Co melting point and, as a consequence, above the Co Curie temperature (1131°C). For the ferromagnetic state, the analysis of the Co/TiC case in Ref. 21 suggests that the effects of magnetism can be understood within a simple rigid-band approach and the Stoner model,[41] in the same way as for Co surfaces.[42] Then to estimate the magnetic corrections to the Co/WC interface energetics, it suffices to have the paramagnetic local density of states of the interface Co layer.

As an assessment of the accuracy of the W pseudopotential used, different bulk properties of W (bcc and fcc), and WC (hexagonal and NaCl) are calculated and compared to the available data from other calculations and experiment. In Table I the data on the lattice parameters, bulk moduli, and cohesive energies are collected. The calculations are done with $8\times8\times8$ Monkhorst-Pack *k*-point meshes. The lattice constant and bulk modulus values are extracted from fits of total energies for different volumes to the Murnaghan equation of state.[48] The cohesive energies are obtained by subtracting the total energies of the spin-polarized free atoms from the total energies of those atoms in bulk.

It is known that the GGA-PW91 gives a significant improvement in the description of the ground-state properties of transition metals over the local-density approximation.[43,49] Although it seemed to give a worse agreement with experiment for $4d$ and $5d$ transition-metal series,[43] it has been shown[49] that this discrepancy is related to the use of the atomic-spheres approximation (ASA). Compared to the local-density approximation (LDA), the GGA-PW91 lowers the cohesive energies and gives larger equilibrium volumes and smaller bulk moduli. The fact that this trend is not much in line with our comparisons in Table I can be attributed to the use of the ASA in many of the referred calculations.

Our result for the equilibrium lattice constant of cubic WC is 4.346 Å. This is overestimated by a few percent compared to the values extracted from experiments. This lattice constant value is close to the calculated value for TiC (4.33 Å).[20] Our result for the cohesive energies of the ground state configurations of W (bcc) and WC (hexagonal) are approximately 0.5 eV higher than for the less stable fcc structures of W and WC, respectively. Our overall conclusion is that all the calculated values are in a reasonably good agreement with the available experimental data and other first-principles calculations.

An important point for our discussion of the interfaces is the difference between WC and TiC electronic structures. The nature of bonding in bulk carbides in the NaCl structure has been investigated by first-principles methods in e.g., Refs. 45 and 50. Reference 45 shows that the bonding in cubic WC and TiC is dominated by covalent bonds between $2p$ orbitals of C and d orbitals of metals, with some additional metallic d-d bonding. This is consistent with our result for the valence electron density in Fig. 1. The density is more uniformly distributed in WC than in TiC. This indicates that WC is a more metallic system than TiC. This is to be expected, since there is a trend toward higher conductivities from semimetallic[51] group-IV carbides to group-V and -VI carbides. It was pointed out earlier that cubic WC has even more metallic bonding nature than the group-V materials.[47]

The trend in metallicity of transition-metal carbides can be understood within a rigid-band model for the density of states developed in Ref. 50. For transition-metal carbides with a NaCl structure, there is typically a broad minimum in the density of states separating bonding and antibonding states, as illustrated by our result for the local density of states (LDOS) in Fig. 2. For TiC with six valence electrons, the Fermi level lies at the bottom of this minimum, indicating a stable structure where the bonding states are filled and the antibonding states are empty [see Fig. 2(c)]. When going from group-IV to group-VI transition-metal carbides, the extra electrons successively fill the antibonding states, leading to increasingly unstable NaCl structures. Compared to TiC, WC has two more valence electrons per unit cell, which fill the antibonding states. For cubic WC the filling of the anti-

TABLE I. Calculations of lattice constants a_0, bulk moduli B, and cohesive energies E_{coh} of bulk W and WC compared with other calculations and experimental (Expt) data. (LCAO is the linear combination of atomic orbitals. FP-LMTO is the full potential linear muffin-tin orbital. LSDA is the local-spin-density approximation.)

Crystal	Method	Source	a_0 (Å)	B (Mbar)	E_{coh} (eV)
W(bcc)	GGA-PWPP	This work	3.16	3.04	8.7
	LSDA-LMTO	Ref. 43	3.21	3.03	~8.9
	GGA-LMTO	Ref. 43	3.25	2.72	~7.8
	LDA-LMTO-ASA	Ref. 44	3.15	2.80	-
	Expt	Quoted in Ref. 44	3.16	3.23	-
	Expt	Quoted in Ref. 43	3.16	3.10	8.92
W(fcc)	GGA-PWPP	This work	4.01	2.83	8.2
WC(hex.)	GGA-PWPP	This work	2.90	4.04	8.5
	LDA-FP-LMTO	Ref. 45	2.88	3.29	9.72
	LDA-LMTO-ASA	Ref. 44	2.83	6.55	-
	LDA-LMTO-ASA	Ref. 46	2.88	4.13	8.90
	LDA-LCAO	Ref. 47	-	-	8.95
	Expt	Quoted in Ref. 44	2.91	5.77	-
	Expt	Quoted in Ref. 45	2.91	3.31	8.34
	Expt	Quoted in Ref. 46	-	4.34	-
	Expt	Quoted in Ref. 46	-	4.43	-
	Expt	Quoted in Ref. 46	-	-	8.35
WC(fcc)	GGA-PWPP	This work	4.35	3.50	8.0
	LDA-LCAO	Ref. 47	4.32	3.90	8.50
	LDA-FP-LMTO	Ref. 45	4.29	3.19	9.46
	LDA-LMTO-ASA	Ref. 44	4.22	3.75	-
	Expt	Quoted in Ref. 47	4.220	-	-
	Expt	Quoted in Ref. 47	4.229	-	-
	Expt	Quoted in Ref. 47	4.266	-	-
	Expt	Quoted in Ref. 47	-	4.0-4.3	-

bonding states gives relatively large LDOS at the Fermi level, as can be seen in Fig. 2(b), and as previously discussed in, e.g., Ref. 45.

In Table I we calculate the cohesive energy of 8.0 eV/atom for cubic WC to be compared to the calculated cohesive energy of 7.3 eV/atom for TiC.[20] Since the extra filling of the antibonding states in WC should reduce the contribution of the carbon-metal *p-d* bonds, the higher value for WC is an extra indication of a stronger W-W metallic bond in WC.

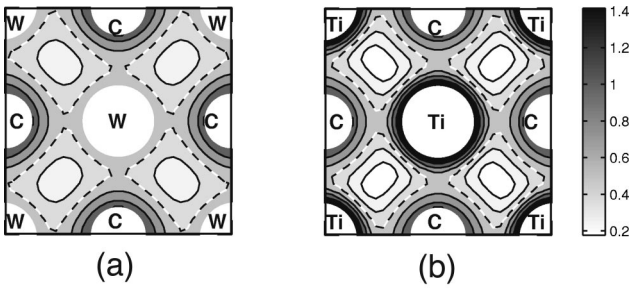

FIG. 1. Contour plots of valence charge density in (001) cuts of bulk WC and TiC. The dashed line is a $+0.5$-electron/Å^3 reference level, and the consecutive contours change by a factor of $\sqrt{2}$.

B. Co/WC interface

To our knowledge, the atomic structure of Co/WC interfaces has not been characterized experimentally. The only relevant information available is the shapes of carbide crys-

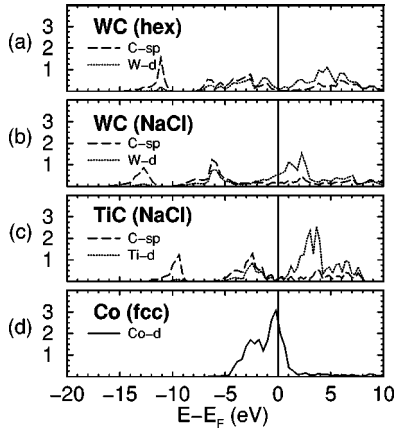

FIG. 2. Main components of the local density of states (LDOS) projected onto atomic orbitals for hexagonal (a) and cubic (b) WC, cubic TiC (c), and fcc Co (d) bulk materials. The vertical solid lines show the position of the Fermi energy.

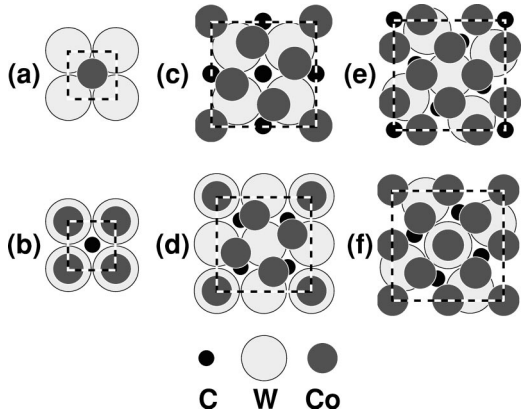

FIG. 3. Atomic structures modeling the Co/WC interface. The relative positions of Co, W, and C atoms in the interface layers are shown. The notations are, from left to right, 1Co/1WC-I (a) and -II (b), 5Co/4WC-I (c) and -II (d), and 8Co/5WC-I (e) and -II (f).

tals embedded in a metal binder in hard metals (see, e.g., Refs. 16 and 38). In cemented carbides, WC grains are typically found in the form of triangular prisms embedded in the metal binder phase. The Co/WC orientation relationship behind this shape is expected to be connected to the hexagonal structure of WC, and hence should not be transferable to the cubic carbide case considered here. Cubic carbide grains tend to develop a cubic shape, angular or rounded to a different extent, depending on the composition of the carbide and the binder metal.[38] This shape behavior makes the {001}//{001} interface orientation relationship a very realistic assumption.

Since both β-WC and TiC have NaCl structures, we can model the Co/WC interface by the same set of high-symmetry configurations as for Co/TiC in Ref. 20. To create the interface model systems, we match unit cells of different sizes in the (100) surfaces of Co and WC together. In this process, the lattice constant of WC is kept fixed, and the Co matrix is stretched to obtain coherent structures. The unit cells are chosen as to minimize the induced strain energy, but are at the same time kept small for computational reasons. This gives three different interface unit cells; 1Co/1WC, 5Co/4WC and 8Co/5WC. The notation used is mCo/nWC, where m/n is the relative number of Co atoms compared to W and C atoms within one unit cell. For each of these configurations, there are two independent high-symmetry translation states, denoted as mCo/nWC-I and mCo/nWC-II, respectively. The model systems used are shown with notations in Fig. 3. We also take into account that the in-plane stretch of the Co lattice induces a bulk relaxation effect of the Co interlayer distances. In the perpendicular direction the interfaces are modeled as periodic sequences of alternating Co and WC slabs, with each supercell containing one Co slab and one WC slab without any vacuum layers.

Using these model systems, we analyze the energetics of the Co/WC interface. Unfortunately, it is very difficult to obtain experimental information of the energetics of a buried interface and the only experimental data available are values of the work of separation (adhesion) from sessile drop wetting experiments. The work of separation, W_{sep}, is the work required to reversibly separate the interface into two free surfaces, neglecting diffusional and plastic degrees of freedom.[1] These dissipative processes dictate that W_{sep} is a lower bound to the actual work measured in a cleavage experiment. In addition to the possible connection to experiment, the usefulness of the work of separation in our analysis is also in that it is quite a direct measure of the interface bond strength. The work of separation can be calculated as the difference in total energy between a system in which the surfaces are free to another in which they are in contact, forming the interface. With the slab geometry, this can be expressed as

$$W_{sep}=(E_1+E_2-E_{12})/2A. \quad (1)$$

Here E_{12} is the total energy of the interface system, and E_1 and E_2 are the total energies of the separated slabs calculated in the same-size supercells. A is the interfacial area and the factor 2 accounts for the two identical interfaces in the supercell.

Another important quantity is the interface energy γ. The interface energy can be viewed as the work required to create the interface from bulk materials. In contrast to the work of separation, it is not an absolute measure of the interface bond strength. Instead it compares the interfacial bonds to the bonding in the bulk material. Thermodynamically, γ is the excess free energy of the interface, and is a crucial parameter in the process of precipitation. The precipitation kinetics is influenced by the interfacial free energy between the precipitate phase and the matrix phase. Therefore, it should be an important parameter in the formation of the carbide grains in the metal matrix during sintering in which the grains obtain their characteristic shape. It has been proposed that the resulting shape of the carbide crystals in cemented carbides is determined by a balance of relaxation and growth processes in which the carbide atoms are dissolved and reprecipitates on the same or another crystal.[38]

The interface energy can be calculated by subtracting from the total energy of the interface system the total energies of the corresponding bulk phases,

$$\gamma=(E_{12}-E_{1,bulk}-E_{2,bulk})/2A=\sigma_1+\sigma_2-W_{sep}, \quad (2)$$

and can also be expressed as the difference between the surface energies $\sigma_{1,2}$ of the two slabs, and the work of separation W_{sep}.

All total-energy calculations are performed using supercells with three layers of each material [(3+3)-layer supercells]. The Brillouin zones are sampled with $8\times8\times2$, $4\times4\times2$, and $2\times2\times2$ k-point grids for the 1Co/1WC, 5Co/4WC and 8Co/5WC interfaces, respectively. The plane-wave cutoff energy is 26 Ry. Convergence tests are done with respect to the number of layers, the k-point sampling and the plane wave cutoff energy as shown in Fig. 4. The dominating source of the convergence error is the convergence with respect to the number of layers. For the important case of the 1Co/1WC-I system this error is within 0.05 J/m^2. As the more complex interface systems can be considered mixtures of the 1Co/1WC-I and 1Co/1WC-II systems, we expect the convergence error for them of about 0.1 J/m^2. These conver-

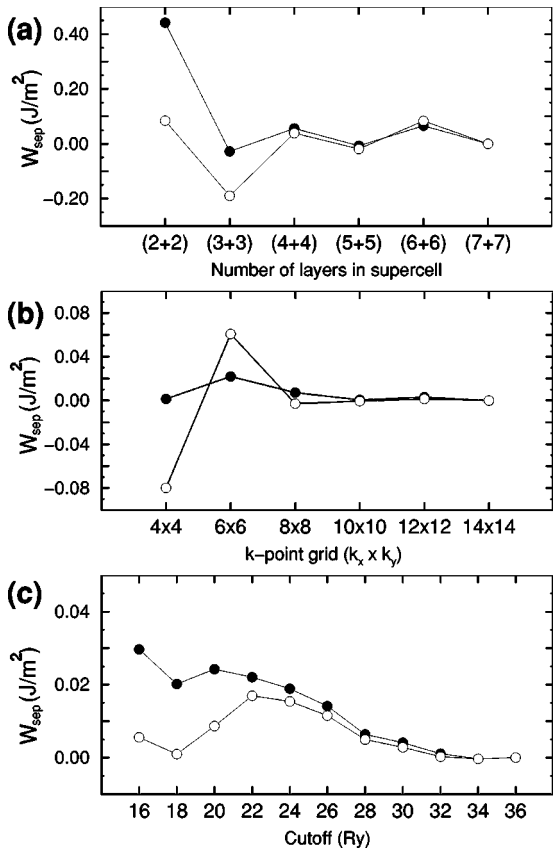

FIG. 4. Convergence of the work of separation for the two 1Co/1WC interfaces with respect to (a) the number of layers in each of the slabs in the supercell, (b) the *k*-point sampling, and (c) the plane-wave cutoff energy. Filled and unfilled circles correspond to the 1Co/1WC-I and 1Co/1WC-II interfaces, respectively. The work of separation is counted from the final point in each figure. In (b), a Monkhorst-Pack grid $k_x \times k_y \times k_z$ with $k_z = 2$ is used.

gence tests show that the work of separation is adequately converged with the chosen basis.

Both relaxed and unrelaxed values are calculated for all model systems. In the relaxed calculations, all atoms in the interface layers are allowed to relax in all directions. The atomic positions of one middle layer of each slab and the supercell volume are kept fixed. The unrelaxed values of the work of separation are calculated with respect to unrelaxed free slabs.

The results for the work of separation for the Co/WC interface are summarized in Table II together with the optimized interlayer distances *d* between the Co and WC slabs. Since the lattice constants of WC and TiC are close, the interlayer distances in the Co/WC supercells are practically the same as in the Co/TiC ones.[20] The table also includes the difference in W_{sep} between the Co/WC and the corresponding Co/TiC interfaces. The relaxed values for the 5Co/4WC and 8Co/5WC model systems are about 3.7 J/m^2. This is close to the wetting experimental value of 3.82 J/m^2.[52] Compared to the work of separation for the Co/TiC interface, it is approximately 0.4 J/m^2 higher. This means that we reproduce the experimental trend of better wetting for Co on WC than on TiC, although the experimental difference is

TABLE II. Work of separation W_{sep} for the Co/WC interface compared to the Co/TiC interface. There are values for both unrelaxed (Unrel) and relaxed (Rel) structures. Here *d* is the optimized interlayer distance between the Co and WC slabs, and ΔW_{sep} is the difference between the given values of W_{sep} for Co/WC and the corresponding values for Co/TiC from Refs. 19 and 20.

Interface	d(Å)	W_{sep} (J/m^2)		ΔW_{sep} (J/m^2)	
		Unrel	Rel	Unrel	Rel
1Co/1WC-I	1.80	5.20	4.50	0.78	0.32
1Co/1WC-II	2.37	2.49	1.58	1.81	1.12
5Co/4WC-I	2.08	3.61	3.53	0.87	0.25
5Co/4WC-II	2.08	3.60	3.67	1.00	0.42
8Co/5WC-I	2.13	3.68	3.69	1.02	0.44
8Co/5WC-II	2.13	3.67	3.65	1.00	0.43

about half this value.[52] As pointed out in Ref. 1, such a comparison can only be semiquantative, due to a difference in the definitions of the ideal work of separation and the experimentally measured work of adhesion.

The work of separation is almost unaffected by relaxation in the case of Co/WC, while there is a large relaxation effect for Co/TiC. The relaxation effect at the Co/WC interface is compensated by a similar relaxation for the free Co and WC surfaces resulting in an effective cancellation in the W_{sep} value. The comparison of the perpendicular relaxations of the symmetry independent atoms at the Co/WC and Co/TiC interfaces is given in Fig. 5. The relaxation of the atomic coordinates is similar in the two systems, except the large relaxation of some of the C atoms at the Co/TiC interface. The two atoms with the pronounced relaxations are the atom in the middle of the unit cell in Fig. 3(c) and the corner atom in Fig. 3(e), at 5Co/4TiC-I and 8Co/5TiC-I interfaces, respectively. Both these atoms are centered under four Co atoms allowing for a strong Co-C bonding that can counteract the Ti-C bonding. This effect is not sufficiently strong at the Co/WC interface to give the same large relaxations. This is

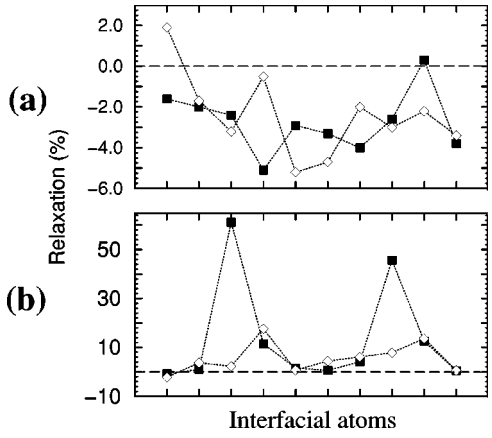

FIG. 5. Perpendicular relaxation of the W(Ti) (a) and C (b) atoms in different positions at the Co/WC (diamonds) and Co/TiC (filled squares) interfaces expressed in percent of the bulk W(Ti)C interlayer distances. Note the difference in scale between (a) and (b).

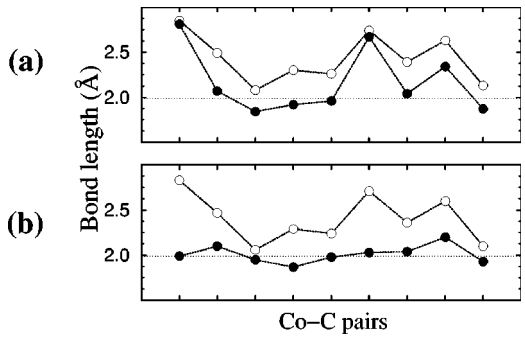

FIG. 6. Unrelaxed (unfilled circles) and relaxed (filled circles) Co-C bond lengths in Å for different Co-C pairs at the Co/WC (a) and Co/TiC (b) interfaces. Only Co-C pairs at the 5Co/4W(Ti) and 8Co/5W(Ti) interfaces are displayed. The horizontal dot lines indicates the sum of the Co and C covalent radii.

indicated more explicitly in Fig. 6, which shows the Co-C bond lengths for different Co-C pairs at the Co/WC and Co/TiC interfaces. The variation in the Co-C distance is much smaller at the relaxed Co/TiC interface, where the equilibrium bond distances are attained. The Co/TiC interface Co-C bond length is close to the sum of the Co and C covalent radii [2.0 Å (Ref. 53)] throughout, which is not the case at the Co/WC interface.

The 1Co/1W(Ti)C systems are associated with a large induced strain energy originating from the stretch of the Co lattice to obtain a coherent interface. They can nevertheless give valuable information about the bonding mechanisms at the metal-ceramic interface. The two translation states 1Co/1W(Ti)C-I and -II correspond to interfaces where the Co atoms are over the C and W sites, respectively. At a more complex interface, represented by the 5Co/4WC and 8Co/5WC model systems, the probability for a Co atom being close to a C atom is about the same as being close to a W atom. It is reasonable to believe that such interfacial structures can be viewed as superpositions of the local environments provided by the simple 1Co/1W(Ti)C systems. For instance, it can be seen from Table II that the values of work of separation for the more complex model systems are close to the average values of the two 1Co/1W(Ti)C translation states.

A comparison of the work of separation for the two 1Co/1W(Ti)C interfaces gives an insight into the differences in the interface interactions between the Co/WC and Co/TiC cases. The difference in the work of separation between the two translation states is large for both 1Co/1WC and 1Co/1TiC. This is due to the presence of strong covalent Co-C bonds,[20] although a somewhat similar effect can originate from metal-metal bonds, as for metals on MgO(001).[54] However, the effect of shifting the interfacial Co atoms from C sites to W(Ti) sites is much larger for Co/TiC than for Co/WC (see Table II). Going from 1Co/1WC-I to 1Co/1WC-II, the work of separation decreases by approximately a factor of 3, while the work of separation for 1Co/1TiC-I is almost an order of magnitude larger than for 1Co/1TiC-II. This means that the interfacial covalent Co-C bonds play a more important part in the interface adhesion in the case of Co/TiC, and is an indication that the metal-metal contribution to the adhesion is larger for Co/WC than for Co/TiC.

TABLE III. Interface energies γ at the Co/WC interface compared to the Co/TiC interface. The energies are given for both unrelaxed (Unrel) and relaxed (Rel) structures. Here $\Delta\gamma$ is the difference between the given values of γ for Co/WC and the corresponding Co/TiC values of Ref. 20.

Interface	γ (J/m^2)		$\Delta\gamma$ (J/m^2)	
	Unrel	Rel	Unrel	Rel
1Co/1WC-I	-0.49	-0.53	-0.70	-0.73
1Co/1WC-II	2.24	2.40	-1.71	-1.51
5Co/4WC-I	0.96	0.35	-0.73	-0.61
5Co/4WC-II	0.97	0.21	-0.86	-0.77
8Co/5WC-I	1.08	0.44	-1.03	-0.96
8Co/5WC-II	1.09	0.48	-1.02	-0.95

The relaxed and unrelaxed values of the Co/WC interface energy are given in Table III together with the difference in interface energy $\Delta\gamma$, compared to Co/TiC. There is a large variation in $\Delta\gamma$ over the different model systems. Thus the interface energy is more sensitive than the work of separation to structural variations in these metal-ceramic interfaces. The relaxation effects of the interface energy is almost the same at the Co/WC and Co/TiC interfaces, but the interface energy is about 1 J/m^2 higher for Co/TiC. The fact of a much lower value of the interface energy for Co/WC than for Co/TiC implies that the formation of Co/WC interfaces is energetically more favorable in the WC-Co cemented carbide than the formation of the Co/TiC interfaces in the Co-TiC cermet.

For a more detailed understanding of the interfacial interatomic interactions, a close study of the electronic structure

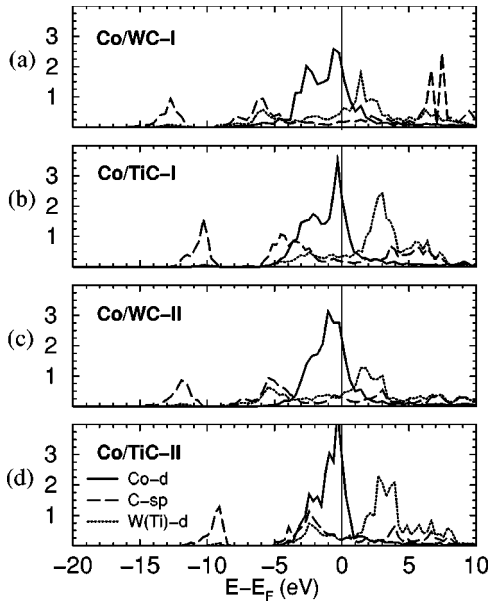

FIG. 7. Main components of the local density of states projected onto atomic orbitals for the 1Co/1W(Ti)C-I interfaces in (a) and (b), and for the 1Co/1W(Ti)C-II interfaces in (c) and (d). The vertical solid line indicates the Fermi energy.

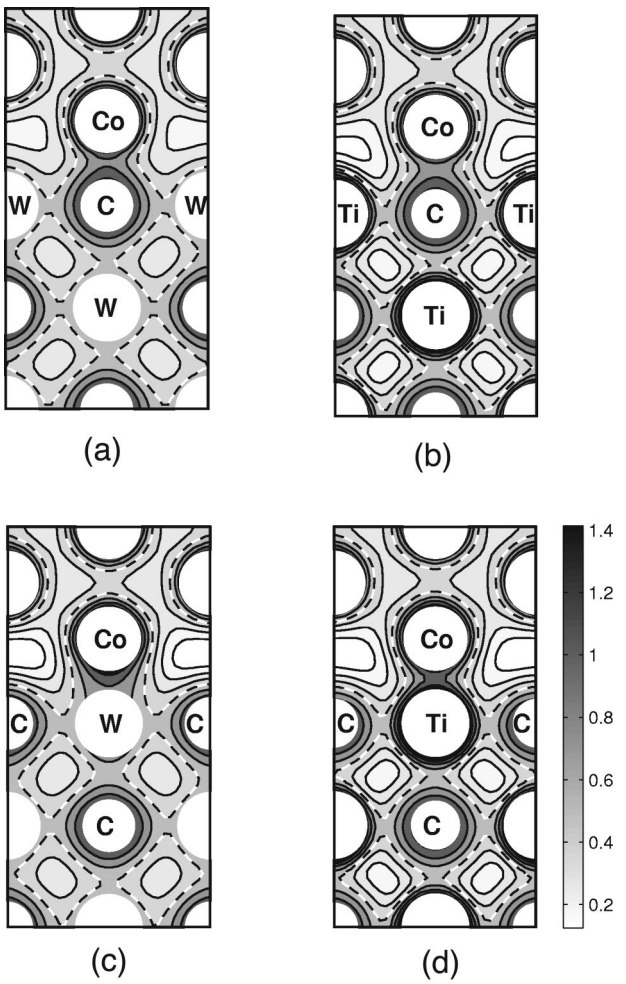

FIG. 8. Contour plots for (010) cuts of the valence electron density at 1Co/1WC-I (a), 1Co/1TiC-I (b), 1Co/1WC-II (c), and 1Co/1TiC-II (d) interfaces (unrelaxed, 5+5-layer supercells). The dashed line is a $+0.5$-electron/Å^3 reference level, and the consecutive contours change by a factor of $\sqrt{2}$.

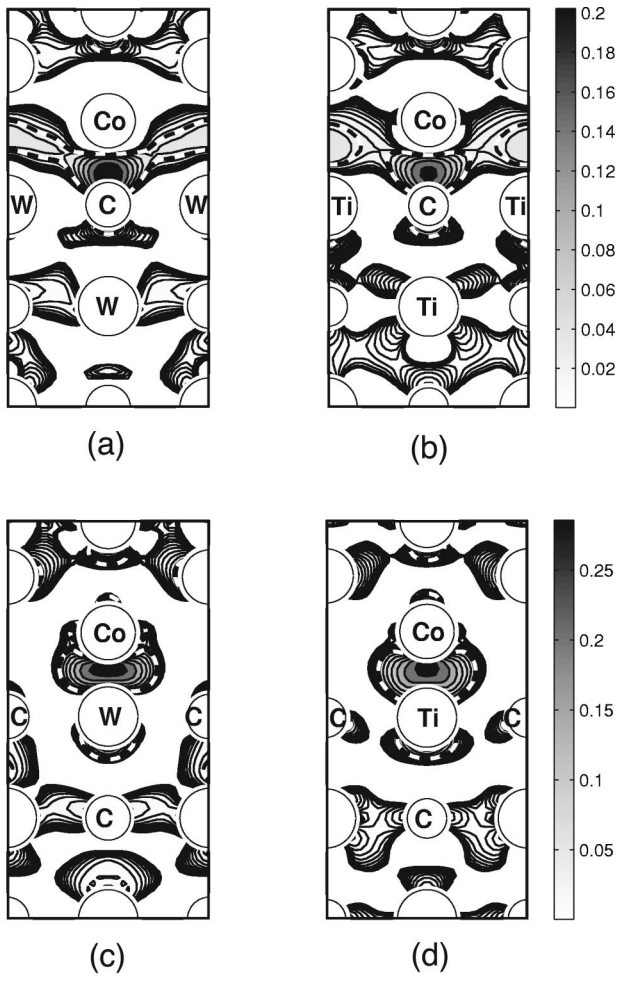

FIG. 9. Induced valence electron density when free unrelaxed Co and W(Ti)C slabs are put together to form unrelaxed 1Co/1WC interfaces. The 1Co/1W(Ti)C-I interfaces are displayed in (a) and (b), and the 1Co/1W(Ti)C-II interfaces in (c) and (d). Note the difference in scale between the 1Co/1W(Ti)C-I and 1Co/1W(Ti)C-II figures. Only the regions of charge accumulation are shown. The contour plots are for (010) cuts. The thick dashed line is a 0.03-electron/Å^3 reference level, and consecutive contours change by a factor of $\sqrt{2}$.

is needed. For this purpose, we calculate the LDOS projected onto atomic orbitals for atoms at the 1Co/1WC interface. The projected LDOS at the 1Co/1W(Ti)C-I,II interfaces are shown in Fig. 7. In case of Co/TiC the main mechanism of the interface adhesion is the strong covalent σ bonding between the Co-3d and C-2p orbitals.[19,20] When going from Ti to W, the addition of two extra electrons per carbide pair cause a shift of the C and W states down in energy and away from the region of the Co d band. This should lead to weaker Co-C covalent bonds at the Co/WC interface compared to the Co/TiC interface, in the same way as going from Co/TiC to Co/TiN.[20] If the strength of the Co-C bonds is expected to decrease, then a reasonable explanation for the increase in the work of separation is a higher contribution of the Co-W metal-metal bonding at the Co/WC interface. This is in line with our above analysis of the work of separation site dependence, as well as with the higher metallicity of WC, reflected in its high LDOS around the Fermi level.

There is a significant difference between the Co/WC and Co/TiC cases in how the presence of the interface affects the bonds inside the W(Ti)C slabs. At the 1Co/1TiC-I interface the Co-C p-d hybridization partially destroys the resonance peaks from the Ti-C bonding.[19,20] There is practically no such effect in the Co/WC case. The LDOS in the region of the W-C bonding states in Figs. 7(a) and 7(c) is almost the same as in bulk WC in Fig. 2(b).

Figure 8 shows the valence charge density at the 1Co/1W(Ti)C-I and 1Co/1W(Ti)C-II interfaces. There is a large concentration of charge between the Co atom closest to the interface and the atom underneath, where the interfacial covalent bonds are formed. There is also a higher electron density in the regions between the interface Co and W atoms than between the Co and Ti ones. This suggests that the extra electrons in the Co/WC system take part in a metallic interface bonding.

The change in the electron density when forming the interfaces is presented in Fig. 9, which shows the differences

between the valence electron densities of the unrelaxed interfaces and the corresponding free slabs calculated in the same-size supercells. Only the regions of charge accumulation are displayed. The induced density between Co and W is slightly higher than between Co and Ti, for both the 1Co/1W(Ti)-I and 1Co/1W(Ti)-II interfaces, consistent with our conclusion about larger contribution of the metal-metal bonding at Co/WC than at Co/TiC.

III. CONCLUSIONS

We have performed an *ab initio* study of the Co/WC interface using total-energy density-functional theory calculations. The Co/WC interface energetics is analyzed via the concepts of work of separation and interface energy using a set of model interface geometries. The bonding at the interface is discussed in terms of electronic structure and the results are compared to those of the preceding Co/TiC study. Our values for the work of separation are consistent with the experimental fact of better wetting in the Co/WC system than the Co/TiC one.

We have clarified the differences in the interface interactions between the Co/WC and the Co/TiC interfaces. Both systems are characterized by strong covalent Co-C bonds, originating from the σ-pd-hybridization. Compared to TiC, WC has two more electrons per metal-carbon pair, which cause a shift of the C-sp and W-d states downward, away from the Co-d states. This should reduce the Co-C interaction at the Co/WC interface. The higher adhesion energy of the Co/WC system is a consequence of a larger contribution of metal-metal bonding at the interface, as reflected in the site dependence of the work of separation, as well as in the behavior of the local density of states and the electron density.

Our results for the interface energy show that the Co/WC system has a noticeably lower interface energy than Co/TiC, which can affect the substance redistribution and microstructure during sintering of the cemented carbide. A low interface energy favors the formation of metal-carbide interfaces during the sintering, when the carbide atoms dissolve into the binder phase and then reprecipitate in the growth process of the carbide crystals.

The combination of a low interface energy and a high work of separation, giving a high wettability of the binder phase to the carbide grains, should lead to a reduction in the porosity of the cemented carbide. If introducing defects in the manufacturing of the cemented carbide can be reduced, one can also expect an increase of the material toughness.

As a final comment, we note that the strong directional covalent bonds in the TiC-Co system on the one hand and a more metallic WC-Co system on the other is a likely reason why WC-Co cemented carbides can show a plastic deformation while the TiC-Co cermets are more brittle.

ACKNOWLEDGMENTS

The idea of this work originated from discussions with U. Rolander, Sandvik Coromant AB, and H.-O. Andrén, Chalmers. We are also thankful to B.I. Lundqvist and S. Simak for helpful discussions. This work was supported by the Swedish Foundation for Strategic Research (SSF) and the Swedish Research Council for Engineering Sciences (TFR). Allocation of computer time at the UNICC facilities at Chalmers University of Technology and at the National Supercomputer Center at Linköping University is gratefully acknowledged.

*On leave from Institute for Radiophysics and Electronics, National Academy of Sciences of Ukraine, Kharkov, Ukraine.

[1] M. W. Finnis, J. Phys.: Condens. Matter **8**, 5811 (1996).
[2] F. Ernst, Mater. Sci. Eng., R. **14**, 97 (1995).
[3] J. Th. M. Hosson, H. B. Groen, B. J. Kooi, and V. Vitek, Acta Mater. **47**, 4077 (1999).
[4] A. R. Kennedy and S. M. Wyatt, Composites: Part A **32**, 555 (2001).
[5] U. Schönberger, O. K. Andersen, and M. Methfessel, Acta Metall. Mater. **40**, S1 (1992).
[6] Chun Li, Ruqian Wu, A. J. Freeman, and C. L. Fu, Phys. Rev. B **48**, 8317 (1993).
[7] E. Heifets, E. A. Kotomin, and R. Orlando, J. Phys.: Condens. Matter. (Paris) **8**, 6577 (1996).
[8] J. Goniakowski, Phys. Rev. B **58**, 1189 (1998).
[9] I. G. Batirev, A. Alavi, M. W. Finnis, and T. Deutsch, Phys. Rev. Lett. **82**, 1510 (1999).
[10] C. Verdozzi, D. R. Jennison, P. A. Schultz, and M. P. Sears, Phys. Rev. Lett. **82**, 799 (1999).
[11] A. Bogicevic and D. R. Jennison, Phys. Rev. Lett. **82**, 4050 (1999).
[12] R. Benedek, A. Alavi, D. N. Seidman, L. H. Yang, D. A. Muller, and C. Woodward, Phys. Rev. Lett. **84**, 3362 (2000).
[13] Yu. F. Zhukovskii, E. A. Kotomin, P. W. M. Jacobs, and A. M. Stoneham, Phys. Rev. Lett. **84**, 1256 (2000).
[14] M. Kohyama and J. Hoekstra, Phys. Rev. B **61**, 2672 (2000).
[15] J. Hartford, Phys. Rev. B **61**, 2221 (2000).
[16] H. E. Exner, Int. Met. Rev. **24**, 149 (1979).
[17] J. Gurland, Int. Mater. Rev. **33**, 151 (1988).
[18] E. A. Feest, Composites **25**, 75 (1994).
[19] S. V. Dudiy, J. Hartford, and B. I. Lundqvist, Phys. Rev. Lett. **85**, 1898 (2000).
[20] S. V. Dudiy and B. I. Lundqvist, Phys. Rev. B **64**, 045403 (2001).
[21] S. V. Dudiy, Surf. Sci. (to be published).
[22] P. Hohenberg and W. Kohn, Phys. Rev. **136**, B864 (1964).
[23] W. Kohn and L. Sham, Phys. Rev. **140**, A1133 (1965).
[24] R. O. Jones and O. Gunnarsson, Rev. Mod. Phys. **61**, 689 (1989).
[25] J. P. Perdew, J. A. Chevary, S. H. Vosko, K. A. Jackson, M. R. Pederson, D. J. Singh, and C. Fiolhais, Phys. Rev. B **46**, 6671 (1992).
[26] L. Hansen *et al.*, Dacapo-1.30, Center for Atomic Scale Materials Physics (CAMP), Denmark Technical University.
[27] M. C. Payne, M. P. Teter, D. C. Allan, T. A. Arias, and J. D. Joannopoulos, Rev. Mod. Phys. **64**, 1045 (1992).
[28] G. Kresse and J. Furthmüller, Phys. Rev. B **54**, 11 169 (1996).
[29] G. Kresse and J. Hafner, J. Phys.: Condens. Matter **6**, 8245 (1994).
[30] G. Kresse and J. Furthmüller, Comput. Mater. Sci. **6**, 15 (1996).
[31] D. Vanderbilt, Phys. Rev. B **41**, 7892 (1990).
[32] S. G. Louie, S. Froyen, and M. L. Cohen, Phys. Rev. B **26**, 1738 (1982).

[33] H. J. Monkhorst and J. D. Pack, Phys. Rev. B **13**, 5188 (1976).
[34] M. J. Gillan, J. Phys.: Condens. Matter **1**, 689 (1989).
[35] W. H. Press, S. A. Teukolsky, W. T. Vetterling, and B. P. Flannery, *Numerical Recipes in FORTRAN*, 2nd ed. (Cambridge University Press, Cambridge, 1992).
[36] R. V. Sara, J. Am. Ceram. Soc. **48**, 251 (1955).
[37] P. Ronsheim, L. E. Toth, A. Mazza, E. Pfender, and B. Mitrofanov, J. Mater. Sci. **16**, 2665 (1981).
[38] A. V. Shatov, S. A. Firstov, and I. V. Shatova, Mater. Sci. Eng., A **242**, 7 (1988).
[39] P. Ettmayer, H. Kolaska, W. Lengauer, and K. Dreyer, Int. J. Refractory Metals Hard Mater. **13**, 343 (1995).
[40] M. Rettenmayr, H. E. Exner, and W. Mader, Mater. Sci. Technol. **4**, 984 (1988).
[41] E. C. Stoner, Proc. R. Soc. London, Ser. A **154**, 656 (1936).
[42] M. Aldén, H. L. Skriver, S. Mirbt, and B. Johansson, Surf. Sci. **315**, 157 (1994).
[43] M. Körling and J. Häglund, Phys. Rev. B **45**, 13 293 (1992).
[44] V. P. Zhukov and V. A. Gubanov, Solid State Commun. **56**, 51 (1985).
[45] D. L. Price and B. R. Cooper, Phys. Rev. B **39**, 4945 (1989).
[46] A. Y. Liu, R. M. Wentzcovitch, and M. L. Cohen, Phys. Rev. B **38**, 9483 (1988).
[47] A. Y. Liu and M. L. Cohen, Solid State Commun. **67**, 907 (1988).
[48] F. D. Murnaghan, Proc. Natl. Acad. Sci. U.S.A. **30**, 244 (1944).
[49] V. Ozoliņš and M. Körling, Phys. Rev. B **48**, 18 304 (1993).
[50] J. Häglund, A. F. Guillermet, G. Grimvall, and M. Körling, Phys. Rev. B **48**, 11 685 (1993).
[51] L. E. Toth, *Transition Metal Carbides and Nitrides* (Academic, New York, 1971).
[52] L. Ramqvist, Jernkont. Ann. **153**, 159 (1969).
[53] J. A. Dean, *Lange's Handbook of Chemistry* (McGraw-Hill, New York, 1999).
[54] I. Tanaka, M. Mizuno, S. Nakajyo, and H. Adachi, Acta Metall. Mater. **46**, 6511 (1998).